ACS ES&T Water

pubs.acs.org/estwater

Article

# Tellurite Reduction and Extracellular Recovery of Tellurium Nanorods Using Bioelectrochemical Reactors

Benhur K. Asefaw, Huan Chen, and Youneng Tang*

Cite This: *ACS EST Water* 2024, 4, 4579–4590

Read Online

ACCESS | Metrics & More | Article Recommendations | Supporting Information

**ABSTRACT:** Tellurium is a critical mineral for the foreseeable future due to its scarcity and importance in future energy technology. A biocathode of a bioelectrochemical reactor (BEC) was used for the first time to extracellularly reduce $TeO_3^{2-}$ in simulated wastewater to elemental $Te^0$ nanorods, which could potentially be recovered. Scanning transmission electron microscopy revealed that only 2% of the cells on the biocathode contained intracellular $Te^0$ nanorods. In contrast, in the conventional bioreactor, 40% of the cells contained intracellular $Te^0$ nanorods. Raman spectroscopy determined that the $Te^0$ nanorods were trigonal and amorphous $Te^0$. Microbial community analysis showed the dominance of *Pseudomonas*, *Stenotrophomonas*, and *Azospira* phylotypes in the cathode chamber, despite being <8% in the inoculum. They were all putative $TeO_3^{2-}$ reducers due to their known ability to reduce tellurite and transfer extracellular electrons. The $TeO_3^{2-}$ removal efficiency in the BEC reactor reached 97% when the influent $TeO_3^{2-}$ was 5 mg of Te/L. The reactor operating conditions, including the flow rate, the external resistor, and the cation exchange membrane, were optimized. This work demonstrates the potential of BEC reactors for the continuous and green synthesis of $Te^0$ nanorods.

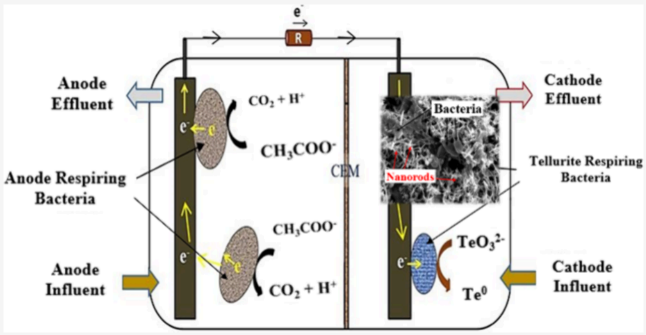


**KEYWORDS:** *biocathode, extracellular tellurium nanorods, resource recovery, scanning transmission electron microscopy, tellurite*



## 1. INTRODUCTION

Tellurium is a scarce metalloid with a crustal abundance of only 5 ppb.[1,2] The stable forms of tellurium in the environment include tellurate ($TeO_4^{2-}$), tellurite ($TeO_3^{2-}$), telluride ($Te^{2-}$), and elemental tellurium ($Te^0$).[3,4] It exists in copper ores as tellurides (i.e., copper telluride ($Cu_2Te$) and silver telluride ($Ag_2Te$)) and gold ores as silvanite ($AgAuTe_4$), calvanite ($AuTe_2$), and chalcogens (i.e., ferrotellurate ($FeTeO_4$), durdenite ($Fe_2(TeO_3)_3{\cdot}4H_2O$), and dunhamite ($PbTeO_3$)).[4−8] During the copper refinery, tellurium as telluride is oxidized in the slimes to sodium tellurite ($Na_2TeO_3$) or sodium tellurate ($Na_2TeO_4$), which can leach into the wastewater.[8,9] Tellurium in wastewater is mainly in the forms of $TeO_3^{2-}$ and $TeO_4^{2-}$ and varies depending on pH and microbial and redox conditions.[10] Tellurium has the potential to harm the kidneys, heart, skin, lungs, neurological system, and gastrointestinal system in rats and people.[11,12] $TeO_3^{2-}$ is generally considered more soluble and toxic than $TeO_4^{2-}$.

Elemental $Te^0$ is commercially produced as a byproduct of copper electrorefining.[7,13] It is commonly used in solar panels,[14−17] thermoelectric materials,[18,19] semiconductors,[20,21] and alloys.[15,22] The growing demand for renewable energy increases the demand for tellurium.[16,19,23] In the 2021 strategy report, the US Department of Energy (DOE) listed tellurium as an "essential" element for the foreseeable future due to its scarcity and importance to future energy technology, emphasizing the importance of tellurium recovery.[24] According to the materials circular economy principles, recovering minor concentrations of critical and economically significant elements such as tellurium is crucial.[15]

Common methods for removing tellurite from wastewater comprise chemical precipitation, adsorption, ion exchange, membrane filtration, and biological reduction.[25−29] Certain microorganisms have the ability to enzymatically reduce tellurite to elemental $Te^0$.[30] Baesman et al. reported growth of *Bacillus selenitireducens* and *Sulfurospirillum barnesii* (*S. barnesii*) using tellurite as an electron acceptor.[31,32] Ramos-Ruiz et al. revealed that a methanogenic consortium exhibited faster tellurite reduction than tellurate to elemental $Te^0$ in batch experiments.[28] A facultative bacterium, *Rhodobacter capsulatus*, was able to produce elemental $Te^0$ nanoparticles outside their cells using malate as an electron donor.[33] *Pseudomonas* sp.[34−36] and *Stenotrophomonas* sp.[37] reduced

Received: June 25, 2024
Revised: August 12, 2024
Accepted: September 13, 2024
Published: September 21, 2024







https://doi.org/10.1021/acsestwater.4c00588
*ACS EST Water* 2024, 4, 4579–4590

Table 1. Operating Conditions of Each Stage in the Main BEC Reactor

| | HRT | | loading rate | | acetate | $TeO_3^{2-}$ | |
|---|---|---|---|---|---|---|---|
| stages | cathode (days) | anode (days) | cathode (mg Te/m$^2$ day) | anode (mg C/m$^2$ day) | anode (mg C/L) | cathode (mg Te/L) | comments |
| I | 1.45 | 1.45 | 660 | 1320 | 20 | 10 | |
| II | 1.45 | 1.45 | 660 | 1320 | 20 | 10 | new CEM[a] |
| III | 1.45 | 1.45 | 660 | 1320 | 20 | 10 | external resistor changed to 1000 Ω |
| IV | 1.93 | 1.45 | 500 | 1320 | 20 | 10 | cathode flow rate reduced to 0.15 L/day |
| V | 2.90 | 1.45 | 330 | 1320 | 20 | 10 | cathode flow rate reduced to 0.10 L/day |
| VI | 2.90 | 1.45 | 165 | 1320 | 20 | 5 | tellurite reduced to 5 mg Te/L |

[a]Note: CEM is cation exchange membrane.

tellurite to elemental $Te^0$ in both extracellular and intracellular ways. Nguyen et al. reported that strains of the *Raoultella* and *Escherichia* genera produced tellurium nanorods both intracellularly and extracellularly.[25] These biological reductions occur in anaerobic conditions and are considered an eco-friendly approach for tellurite removal.[28,38,39]

Biorecovery of elemental $Te^0$ has increasingly gained attention in recent years.[30,40] The biorecovery of elemental $Te^0$ mitigates the risk of secondary contamination and decreases treatment expense, given that tellurium finds broad utility in industries like semiconductors and alloys.[20,24,39] A few studies reported on intracellular production of elemental $Te^0$ from tellurite by microorganisms in conventional bioreactors such as up-flow anaerobic sludge blankets (UASB) and fluidized bed reactors.[3,39,41,42] Retrieving intracellular metal nanoparticles from biomass is an energy- and chemical-intensive process that may lead to further environmental pollution.[43,44] The intracellular nanoparticle separation process involves cell lysis based on lysozyme solution, instruments such as microfluidizers and sonicators for mechanical disruption of the cells, and centrifugation systems for the separation of the nanoparticles. To increase the extracellular reduction of tellurite to elemental $Te^0$, researchers added redox mediators like lawsone and riboflavin into the conventional reactors.[28] This decreased the energy use at the cost of adding chemicals that represent high costs and secondary contamination.[28,33]

Compared to the conventional tellurite-contaminated wastewater treatment processes,[25−29] the bioelectrochemical system (BEC) is an emerging technology with significant potential for simultaneously treating wastewater and recovering resources.[45,46] BEC systems can be categorized into microbial fuel cells, microbial electrolysis cells, microbial electrosynthesis systems, and microbial desalination cells, depending on their application and configuration.[47,48]

BEC reactors are highly efficient, consume less energy, and are safe for the environment.[49] Integrating microbial processes with electrochemical strategies offers benefits such as kinetics-dependent process yields, recovery, and low carbon footprint.[50] The redox potentials for contaminants treated at the cathode are critical in selecting a proper BEC reactor.[48,51] Under anoxic conditions, the degradation of organic matter by exoelectrogens in the anode chamber results in the release of electrons, which are subsequently transported to the cathode electrode via an external circuit to produce energy[52,53] or utilize the energy to reduce high redox potential metals such as $Se^{6+}$ to $Se^0$, $Cr^{6+}$ to $Cr^{3+}$, $Te^{4+}$ to $Te^0$, $Ag^+$ to $Ag^0$, $Cu^{2+}$ to $Cu^0$, and $Co^{2+}$ to $Co^0$ in the cathode.[46,48,50,51,54−58] For instance, in a dual-chamber batch bioelectrochemical system with an abiotic cathode to transform tellurite to $Te^0$, the retrieval of elemental $Te^0$ at the cathode reached 45.3%.[50] The reduction of metals in the cathode is usually based on precious metals such as platinum and titanium as catalysts on the cathode. Biocathode-based BECs use microbes instead of precious metals as the catalyst. Biocathode-based BECs successfully reduced $Se^{6+}$ to $Se^0$, $Cr^{6+}$ to $Cr^{3+}$, and $Co^{2+}$ to $Co^0$.[46,51,54−57]

This study presents a novel approach by evaluating a biocathode-based BEC reactor for the tellurite removal and recovery of extracellular elemental $Te^0$ nanorods, eliminating the need for redox mediators. The biocathode BEC reactor was operated at varied tellurite loading rates to evaluate the regulatory influence on the electrogenic microbial activity for higher extracellular production of elemental $Te^0$ nanorods based on the oxidation−reduction rates. Therefore, the objective of the study is to evaluate the use of the biocathode in the BEC reactor for the extracellular reduction of tellurite to elemental $Te^0$ under various operating conditions.

## 2. MATERIALS AND METHODS

**2.1. Experimental Setup.** Four reactors were operated in a closed mode to eliminate oxygen intrusion: three BEC reactors (Figure S1) and one conventional biofilm reactor (CBR) (Figure S2). The main BEC reactor evaluated the biocathode-based reduction of tellurite to extracellular $Te^0$. The second served as an open-circuit control, and the third BEC reactor was a sterile-biocathode control. Each of the BEC reactors had two 300 mL borosilicate glass chambers (Adams & Chittenden Scientific Glass, USA). A cation exchange membrane (CEM, model CMI-7000, Membrane International, Inc., USA) separated the anode chamber from the cathode chamber of each BEC reactor. The CEM was designed to selectively allow protons ($H^+$) to pass through from the anode to cathode chamber while blocking anions.[59,60] The electrode of each chamber was made of graphite carbon cloth (3 cm × 5 cm, Fuel Cell Store, USA), inoculated with activated sludge from a local wastewater treatment plant except for the cathode of the sterile-biocathode control, and submerged in the liquid media of each chamber. The anode and cathode were connected to an external resistor (100−1000 Ω) with a copper wire. The fourth reactor was a CBR control, which consisted of a column with an inner diameter of 2.2 cm and a height of 9.5 cm packed with plastic media with a specific surface area of 180 $m^2/m^3$ (BioFLO 9, Smoky Mountain Bio Media) for biofilm attachment. Before the system was run, the plastic media in the column of CBR were inoculated with the same microbial consortium as that for the BEC reactors. The temperature for the experiments was at 30 °C.


https://doi.org/10.1021/acsestwater.4c00588
ACS EST Water 2024, 4, 4579−4590

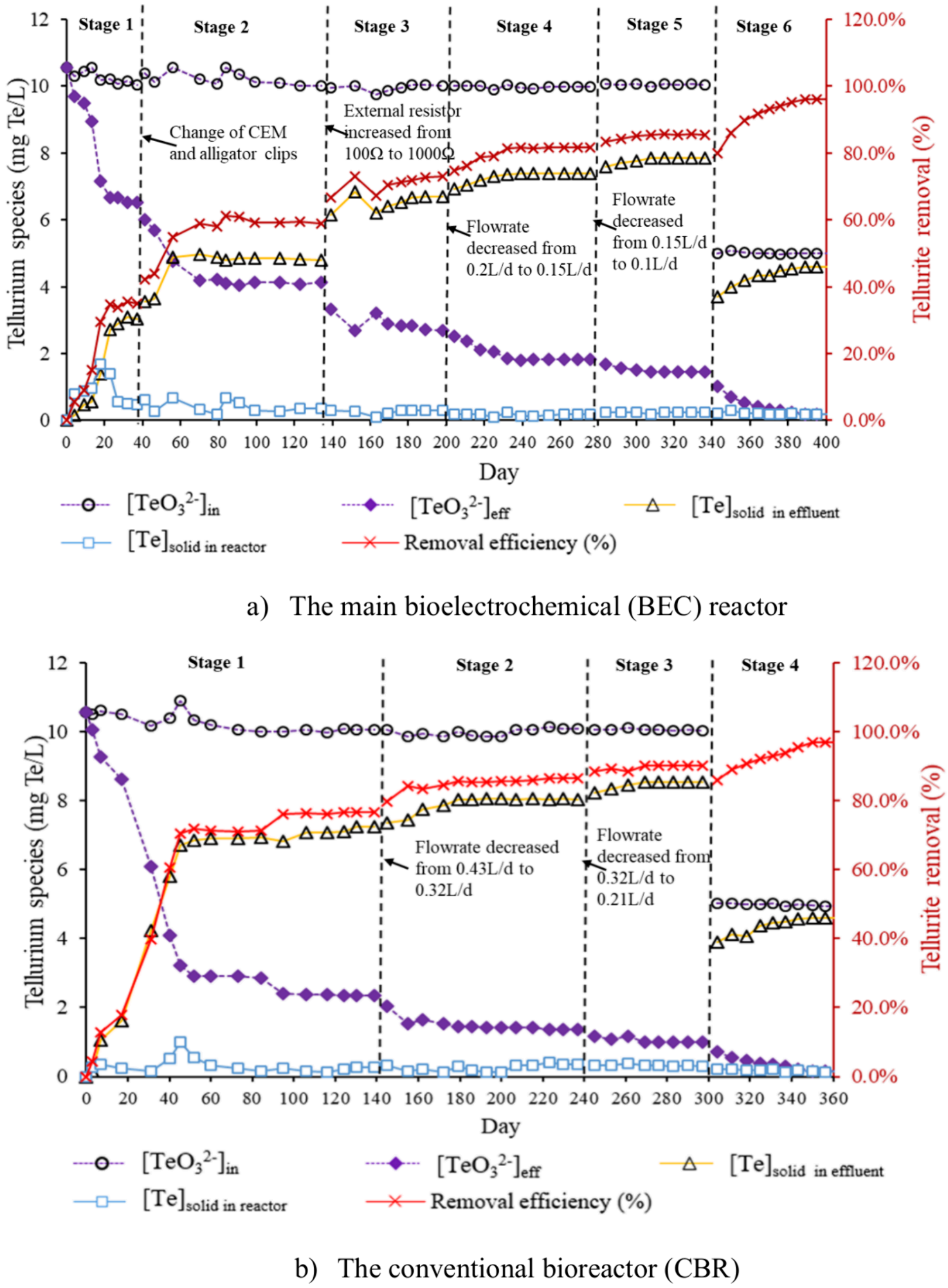


**Figure 1.** Tellurite removal in the cathodic chamber of the main BEC reactor (A) and the CBR (B).

**2.2. Operation of the Reactors.** All reactors were operated in continuous-flow mode. A synthetic mineral medium[46] amended with sodium acetate ($CH_3COONa$) at 20 mg C/L as the sole electron donor was fed to the anode chambers. The experiment was conducted in multiple stages, as indicated in Table 1. The cathode chamber was fed with the same synthetic mineral media amended with potassium tellurite ($K_2TeO_3$) at 5−10 mg Te/L as the sole electron acceptor. Oxygen in the medium was removed by purging nitrogen gas into the medium for 40 min. The pH of the medium was adjusted to 7.0 by adding $CO_2$. The hydraulic retention time (HRT) of both chambers of the BEC reactors varied from 1.45 to 2.9 days, leading to flow rates (100−200 mL/day) and tellurite loading rates (165−660 mg Te/$m^2$ day) summarized in Table 1. The tellurite loading rate in the CBR was the same as in the BEC reactors. The CBR was fed with the same mineral medium amended with tellurite and acetate at the same concentrations at flow rates varying from 210 to 430 mL/day in different stages (Table S1). The ratio of carbon to tellurium fed to the reactors was higher than the stoichiometric ratio of 0.25:1 (see the reaction below) to ensure that carbon was not limiting.

$$0.125CH_3COO^- + 0.093TeO_3^{2-} + 0.56H^+ + 0.022NH_4^+ = 0.022C_5H_7O_2N + 0.093Te + 0.103HCO_3^- + 0.037CO_2 + 0.103H_2O$$

**2.3. Sampling and Analysis.** Influent and effluent samples from the four reactors were collected every week. Tellurium species, including $TeO_3^{2-}$ (dissolved in the influent and effluent) and solid Te (in the effluent and reactor), were



https://doi.org/10.1021/acsestwater.4c00588
ACS EST Water 2024, 4, 4579−4590

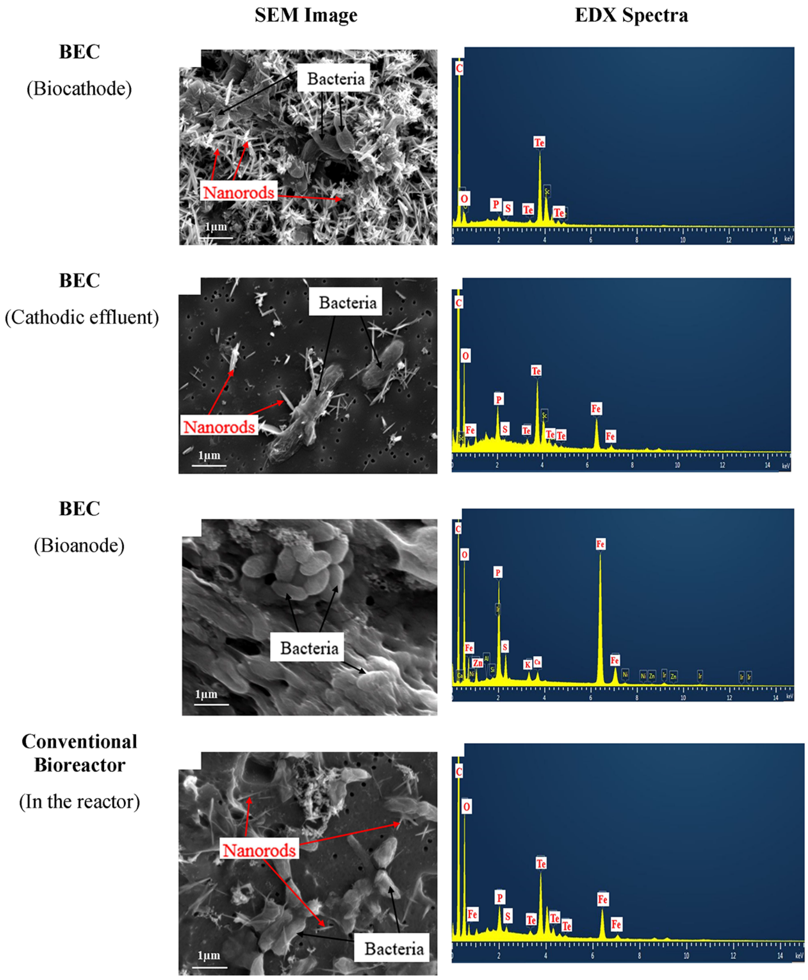


**Figure 2.** Representative SEM images and EDX spectra for the particles sampled from the biocathode (30 images), the cathode effluent (30 images) of the main BEC reactor, the bioanode (30 images), and the conventional reactor (30 images). Note: Images were taken at a steady state of stage 5 for the BEC reactor and stage 3 for the CBR reactor.

quantified. $TeO_3^{2-}$ was measured using a UV−vis spectrophotometer (UV-2501 PC, Shimadzu) as described by Turner et al.[61] with a quantification limit of 20 μg Te/L. The absorbance of $TeO_3^{2-}$ was recorded at the wavelength of 340 nm. The concentration of solid Te in the effluent was calculated as the difference between total tellurium and total soluble tellurium in the effluent sample. The total tellurium was measured by a microwave plasma−atomic emission spectrometer (4100 MP-AES, Agilent Technologies, USA) with a quantification limit of 6.5 μg Te/L. The total soluble tellurium in the effluent sample was measured by the same equipment after the sample was filtered using a 20 nm-pore size syringe and centrifuged for 30 min at 21,000*g*. The difference between total solid tellurium and effluent solid tellurium is the solid tellurium in the reactor. Using ion chromatography (IC, Dionex Aquion ion chromatography system, USA), the acetate and sulfate concentrations were measured with quantification limits of 50 μg C/L and 20 μg S/L, respectively.

Four sets of solid samples were collected at the end of each operating stage from the reactors. In the reactors, solid samples were collected from the bioanode, biocathode, cathode effluent, CBR effluent, and plastic media inside the CBR. In the effluent, solid samples were collected by filtering the effluent from the cathode and CBR through 100 nm membrane filters. From the four sets of samples collected from each location, the first set was analyzed using scanning electron microscopy (SEM, FEI Nova 400 Nano SEM, FEI, USA) with energy-dispersive X-ray spectroscopy (EDX). The second set was analyzed by Raman spectroscopy (Renishaw inVia Raman spectroscopy Leica DM 2500M, Renishaw, USA) at a laser excitation line of ∼638 nm wavelength. The third set was thin-sectioned, stained with osmium (aqueous) for higher contrast, and placed on square mesh copper grids for annular dark-field scanning transmission electron microscopy (STEM, JEMARM200cF, USA) coupled to EDX. The fourth set was used for microbial community analysis. The Illumina MiSeq sequencer (MiSeq, Illumina, USA) was used to analyze the 16S rRNA gene-targeted amplicon sequencing and followed a two-step PCR amplification protocol modified from Pylro et al.[62] and Ionescu et al.[63] The conserved V4 regions of the bacterial 16S rRNA gene were amplified using the forward primer 515F (5′-GTGCCAGCMGCCGCGG-3′) and reverse 806R (5′-GGACTACHVGGGTWTCTAAT-3′). A total of 320,130 sequences resulted from the MiSeq runs of the seven samples. Raw sequences were joined, demultiplexed, and subsequently quality-filtered using QIIME version 1.8.[64] Heat maps were generated in R with the package Superheat.[65] Details of sample preparation for SEM and STEM imaging and DNA extraction are provided in the Supporting Information (SI).

Under standard conditions, the reduction of tellurite to elemental $Te^0$ has a reduction potential of 0.827 V, and the oxidation of acetate has −0.187 V.[66] The corresponding half- and overall reactions are provided in the SI. Therefore, the redox reaction between tellurite and acetate is thermodynamically favorable. The anode and cathode potentials were measured separately using the Hg/HgO reference electrode (Koslow Scientific Company, USA). The potential difference and current between the two chambers were measured by a multimeter (MU 113, Electronic Resources Ltd., USA) connected to the external resistor. During the steady state of each stage, the power density and Coulombic efficiency were computed to assess the electrochemical performance of the BEC reactor. Details are provided in the SI.

## 3. RESULTS AND DISCUSSION

**3.1. Strategies for Increasing the Tellurite Removal Efficiency.** Figure 1 shows that the tellurite removal efficiency increased from stage 1 to stage 6 in the main BEC reactor and the CBR reactor. In stage 1 (day 0−40), the external resistance was 100 Ω, and the cathodic flow rate was 200 mL/day. The tellurite efficiency gradually increased to ∼35% at a steady state. To increase the tellurite removal efficiency, four strategies were attempted, corresponding to stages 2 to 5, respectively. Stage 2 (day 40−135) started when the alligator clips that held the electrodes were cleaned, and the fouled CEM was replaced with a new one. The tellurite removal increased to ∼52% at the steady state of stage 2. In stage 3 (day 135−200), the internal resistance of the system was determined from the polarization curve (Figure S3C) to be approximately 1000 Ω. To maximize the power density, the external resistance was strategically increased to 1000 Ω to match the internal resistance. This change further increased the tellurite removal efficiency to ∼73% at a steady state. When the flow rate for the cathodic chamber was reduced to 150 and 100 mL/day in stages 4 (day 200−280) and 5 (day 280−340), respectively, the tellurite removal efficiency increased to ∼83 and ∼85%, respectively. In stage 6 (day 340−400), the effects of the influent tellurite concentration were evaluated by decreasing it from 10 to 5 mg Te/L, and the tellurite removal efficiency dramatically increased to ∼97%. Fortunately, the tellurite concentration in wastewater is typically below 5 mg Te/L.[4,29,67] The tellurite was converted to solid tellurium. The majority of the solid tellurium was in the cathode effluent (i.e., from 31% of the influent total tellurium in stage 1 to 95% in stage 6), with approximately 2.0% staying in the reactor. The highest percentage of acetate used at the anode chamber in all those 6 stages was 87% (Figure S4).

The cathode chamber of the two control BEC reactors (sterile biocathode and open circuit) had negligible removal of tellurite (0.01 mg Te/L) (Figure S5), suggesting that tellurite reduction in the BEC reactor depended on electron flow from the anode to cathode, as well as bacteria attached to the cathode as the catalyst. In the CBR control, 77% of tellurite was removed at the steady state of stage 1 (Figure 1B). This removal efficiency increased to 98% after the flow rate was decreased by half and the influent tellurite concentration was decreased by half. The tellurite removal efficiency in the CBR of this study (77−98%) is comparable to the CBR studied in the literature (10−92%).[28,29,39,40] In a UASB reactor run at a hydraulic retention time of 0.6 days and fed with ethanol as the electron donor, 80% of tellurite was removed.[40] The addition of riboflavin to the reactor further improved the production of $Te^0$ nanoparticles. Similarly, 92% of the tellurite was removed in the UASB reactor by Mal et al.[39] That UASB was inoculated with anaerobic granular sludge, fed with lactate as the electron donor, and operated at a hydraulic retention time of ∼0.5 days. The tellurite removal efficiency in the BEC reactor of our study (35−97%) is slightly lower than the tellurite removal efficiency in the CBR reactor of our study (77−98%).

**3.2. Characterization of Biogenic Tellurium.** The SEM images and EDX spectra in Figure 2 show that the nanorods produced at the cathodic chamber of the main BEC reactor and the conventional reactor are elemental $Te^0$ nanorods. No $Te^0$ nanorods were observed on the bioanode of the main BEC reactor (Figure 2), suggesting no tellurite transport from the cathode chamber to the anode chamber. The Raman spectra in Figure 3 and Figure S6 further determine that the nanorods were in the form of trigonal $Te^0$ (120 $cm^{-1}$) and the amorphous form of $Te^0$ (145 $cm^{-1}$).[71,72]

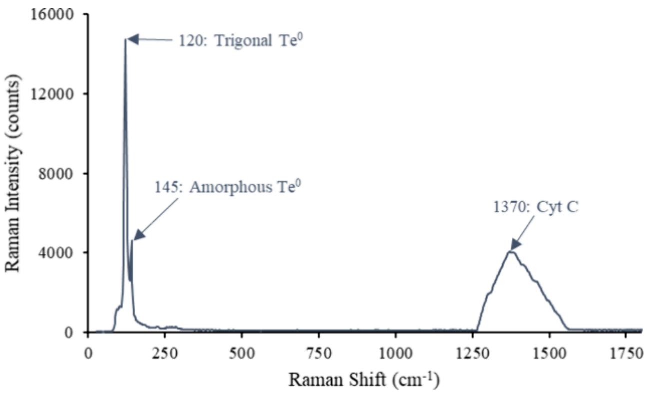


**Figure 3.** Representative Raman spectrum of particle samples on the biocathode. Note: The Raman spectrum was taken at the steady state of stage 5 for the BEC reactor.

Since the white color in the thin-section STEM images perfectly matches the EDX mapping for tellurium in Figure 4, the white color represents $Te^0$ and its location in the particulate samples. The STEM images in Figure 5 and Figure

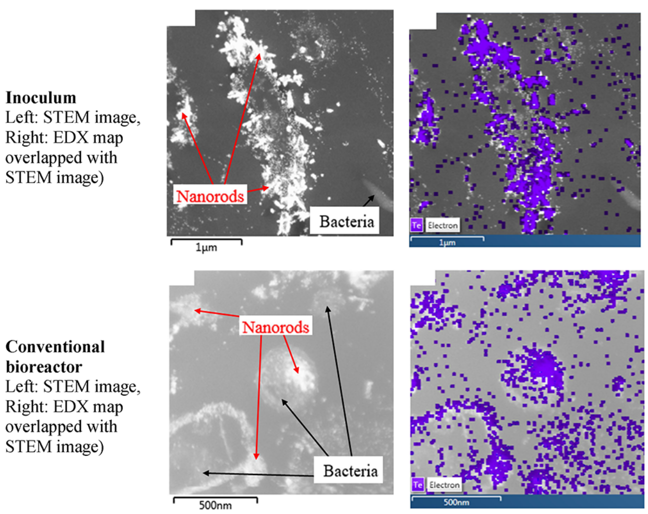


**Figure 4.** Confirmation of white particles as $Te^0$ in thin-section STEM images (left) through overlapping EDX maps (right) with the corresponding STEM images.



https://doi.org/10.1021/acsestwater.4c00588
ACS EST Water 2024, 4, 4579−4590

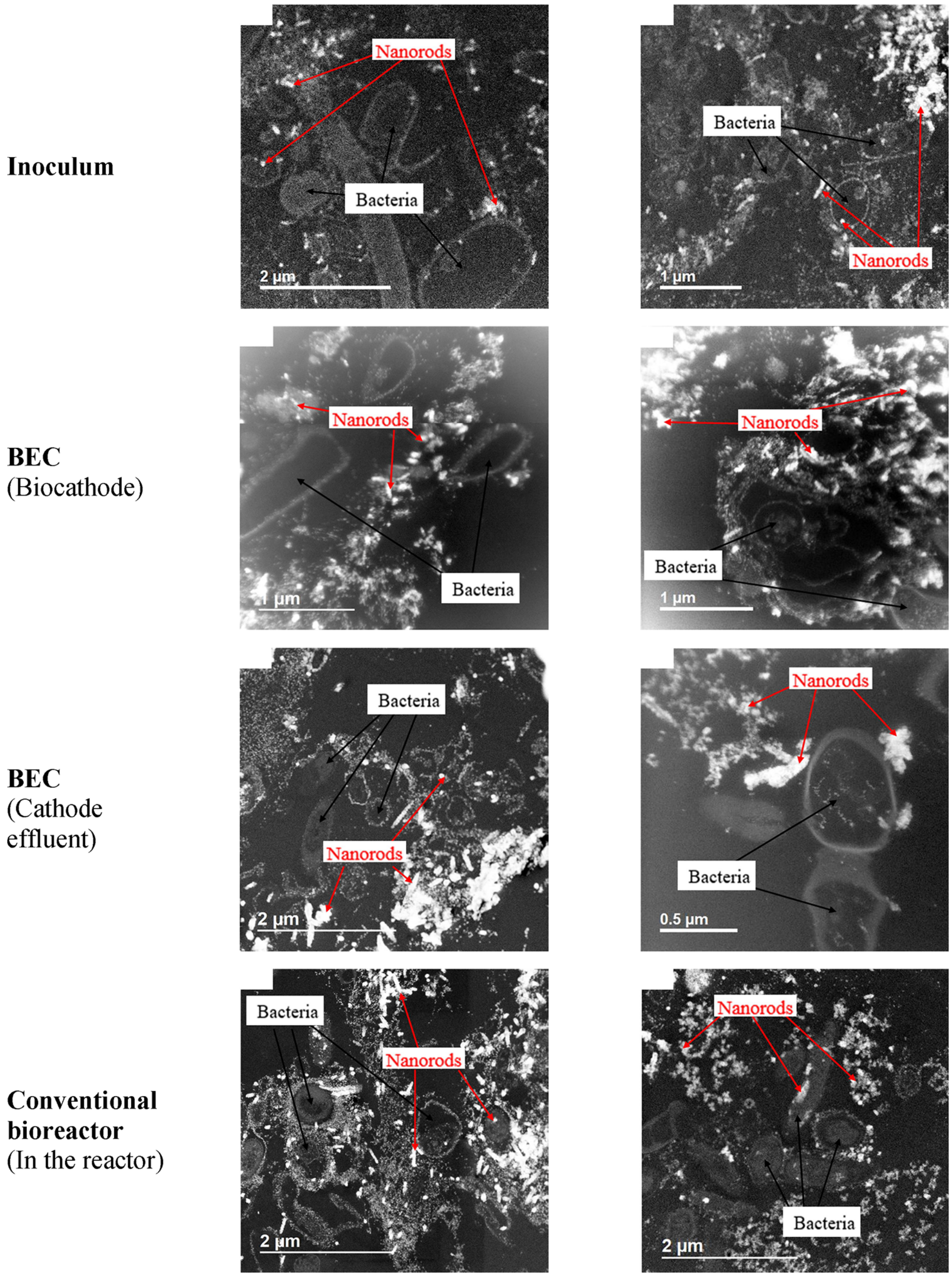


**Figure 5.** Representative thin-section STEM images of particle mixtures in the inoculum, BEC (on the biocathode), BEC (on the cathodic effluent), and conventional bioreactor.

S7 further illustrated that the white color (i.e., $Te^0$ nanorods) is intracellular and extracellular in the inoculum and the CBR reactor but extracellular for the main BEC reactor. On the biocathode of the BEC reactor, less than 2% of the cells contained intracellular $Te^0$ nanorods, whereas in the CBR, ~40% of the cells had intracellular $Te^0$ nanorods (calculated from 30 images). The EDX maps and spectra were collected in the STEM mode with a probe size of 0.12 nm. These nanowire $Te^0$ crystals (<15 nm) aggregated and accumulated onto the surfaces of the bacteria cells. This aggregation was also reported in other studies. Baesman et al. reported irregularly shaped nanospheres (diameter <50 nm) coalescing into larger composite aggregates on the surface of *S. barnesii*.[31] Ramos-Ruiz et al. observed the formation of clusters of $Te^0$ nanorods during the anaerobic reduction of tellurite in a UASB reactor.[28,40] The $Te^0$ nanostructure morphology could be nanorods, nanowires, and nanotubes depending on the microbial species, reaction time, pH, and temperature.[73] Table S2 compares the shapes of the produced $Te^0$ by various bacterial species in various bioreactors. The shape of the elemental $Te^0$ precipitates produced by *Bacillus beveridgei* MLTeJB was nanorods.[74] Pearce et al. reported needle-shaped $Te^0$ by *Geobacter sulfurreducens*.[42] *Bacillus sp.* BZ reduced tellurite to rod-shaped $Te^0$ intracellularly.[75]

In the CBR reactor, the $Te^0$ nanorods were intra- and extracellularly present. Some extracellular $Te^0$ might be originally intracellular and expelled by living cells to reduce Te toxicity for the cells. It is well-known that microbial cells expel intracellular $Te^0$ nanoparticles to reduce its toxicity.[76] Some extracellular $Te^0$ might be from the decay and lysis of


https://doi.org/10.1021/acsestwater.4c00588
ACS EST Water 2024, 4, 4579−4590

cells that contained intracellular $Te^0$. It was also possible that some extracellular $Te^0$ might be directly produced by the microbes. In the BEC reactor, microbes preferred to only produce extracellular $Te^0$ probably because the cells directly got electrons from the cathode and used the electrons to reduce extracellular tellurite to extracellular $Te^0$ through enzymes on the cell surface such as Cytochrome c (Cyt c). By doing this, the microbes did not need to transport the tellurite into the cells and then expel the produced $Te^0$ outside the cell; therefore, the microbes saved energy. The presence of Cyt c on the biocathode sample was found through the Raman peak of 1370 $cm^{-1}$ (Figure 3. Cyt c is a well-known mediator for extracellular electron transfer and metal reduction.[55,77,78]

Compared to the intracellular production of Te nanorods, extracellular production eliminated the need to transfer the electrons and tellurite into the cytoplasm of the microbial cells, which saved energy for the cell and was thereby preferred by the cells on the biocathode of the BEC reactor as shown in Figure S8A. As a result, bacteria enriched on the biocathode preferred to produce extracellular Te nanorods even if they have the ability to produce both intracellular and extracellular Te nanorods. Producing extracellular Te nanorods is more energy-efficient than producing intracellular Te nanorods for microorganisms on the biocathode. On the biocathode, there is less cellular energy cost for transporting $e^-$ and tellurite to the reductase for extracellular Te nanorod production.[55,79] However, this is not necessarily true for a conventional bioreactor. While the tellurite transfer pathway is shorter for the extracellular than intracellular Te nanorod production, the $e^-$ transfer pathway is longer for extracellular than for intracellular Te nanorod production (Figure S8B).[55,80,81]

With the current setup of the BEC reactor, we successfully produced $Te^0$ nanorods primarily outside the microbial cells. Further separation and recovery of the extracellular $Te^0$ nanorods may be achieved through bacteria nanoparticle separators, tangential flow ultrafiltration, and centrifugation. These approaches have been shown effective in previous studies for separation of nanoparticles such as nickel, silver, and selenium nanoparticles from water and biomass.[68−70]

**3.3. Electron Distribution.** Bar charts were used to illustrate the electron distribution in the anode and cathode chambers of the BEC reactor at steady states (Figure 6). Electron sinks in the anode chamber of the BEC reactor included methane production (<1%), sulfate reduction (2.5−3%), generation of electrical current corresponding to the Coulombic efficiency (20−40%), and biomass synthesis and others (57−77%). Electron sinks in the cathode chamber of the reactor included methane production (<1%), sulfate reduction (2.7−6.4%), tellurite reduction to $Te^0$ (∼10%), and biomass synthesis and others (84−91%).

In the experiments, the current density (current normalized to the electrode surface area) and voltage gradually increased to 0.015 $A/m^2$ and 45 mV, respectively (Figure S9). These values are comparable with other anaerobic double-chamber BEC reactors that used nitrate, chromate, and selenate as the electron acceptors (0.003−0.123 $A/m^2$).[46,54,82] The difference between the theoretical and measured cathode overpotentials gave the cathode overpotential loss (−144 mV), as shown in Table S3. This value corresponded to 98% of the total electrode overpotential loss in the reactor (147 mV). This is analogous to the literature: the cathode overpotential loss in the BEC reactor (87%) and microbial fuel cells (83−90%)

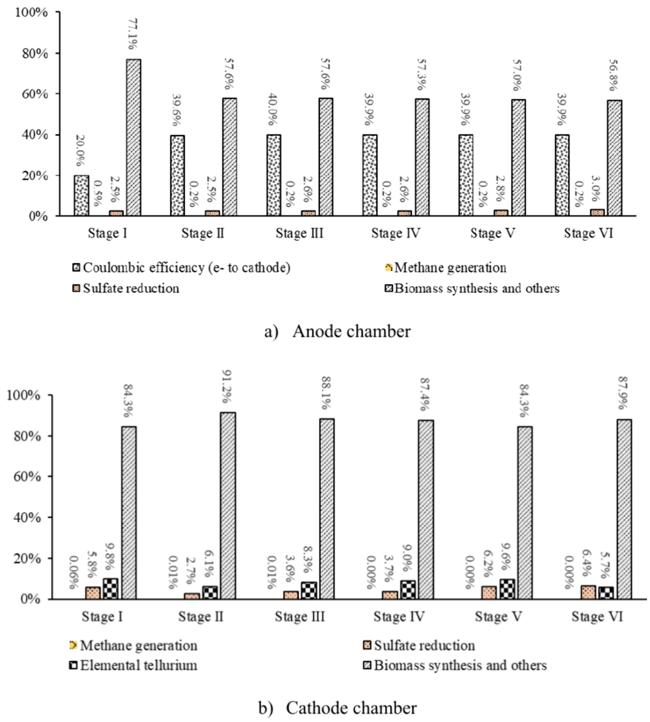


**Figure 6.** Electron distribution in the anode chamber (a) and cathode chamber (b) of the main BEC reactor. Note: The calculation involved in electron distribution is provided in the Supporting Information.

reported in the literature was greater than the anode overpotential loss.[46,83,84]

**3.4. Microbial Community Analysis.** Microbial community analysis was performed on biomass collected from various locations during the steady states of stage 5 (BEC reactor) and stage 3 (CBR reactor). These stages were chosen because both reactors had the highest removal rates at the same surface loading rate for tellurite. Figure 7 shows the relative abundance of the major bacterial genera in samples from the following 7 specific locations: the inoculum, anode, anode effluent, biocathode, biocathode effluent, plastic media in the CBR reactor, and CBR effluent.

The anode of the BEC reactor was predominantly populated by a biofilm consisting of *Geobacter* (30%), *Dechloromonas* (32%), *Acinetobacter* (29%), *Zoogloea* (18%), *Thauera* (17%), *Desulfovibrio* (17%), and *Geothrix* (14%). Interestingly, *Geobacter*, a well-known electroactive bacterium, was found to be among the dominant genera in the inoculum, at both electrodes of the BEC reactor and the CBR reactor. *Geobacter* directly transports electrons from its inner membrane to the anode using its pili.[85,86] *Dechloromonas*, *Acinetobacter*, *Zoogloea*, *Thauera*, and *Geothrix* are also well-known electroactive bacteria.[86−90] *Desulfovibrio*, a well-known sulfate reducer, probably explained the reduction of sulfate in the anode.[91]

The dominant genera on the biomass carrier of the CBR reactor included *Acholeplasma* (19%), *Pseudomonas* (16%), *Magnetospirillum* (15%), *Geobacter* (14%), *Deinococcus* (14%), *Desulfovibrio* (13%), *Stenotrophomonas* (11%), and *Acetinobacter* (10%). Notably, *Pseudomonas*, *Geobacter*, and *Stenotrophomonas* were among the dominant genera in the biocathode. *Acholeplasma*, *Magnetospirillum*, and *Deinococcus* are also known to produce $Te^0$.[92−94]

The predominant genera on the biocathode of the BEC reactor were *Pseudomonas* (33%), *Stenotrophomonas* (29%),


https://doi.org/10.1021/acsestwater.4c00588
ACS EST Water 2024, 4, 4579−4590

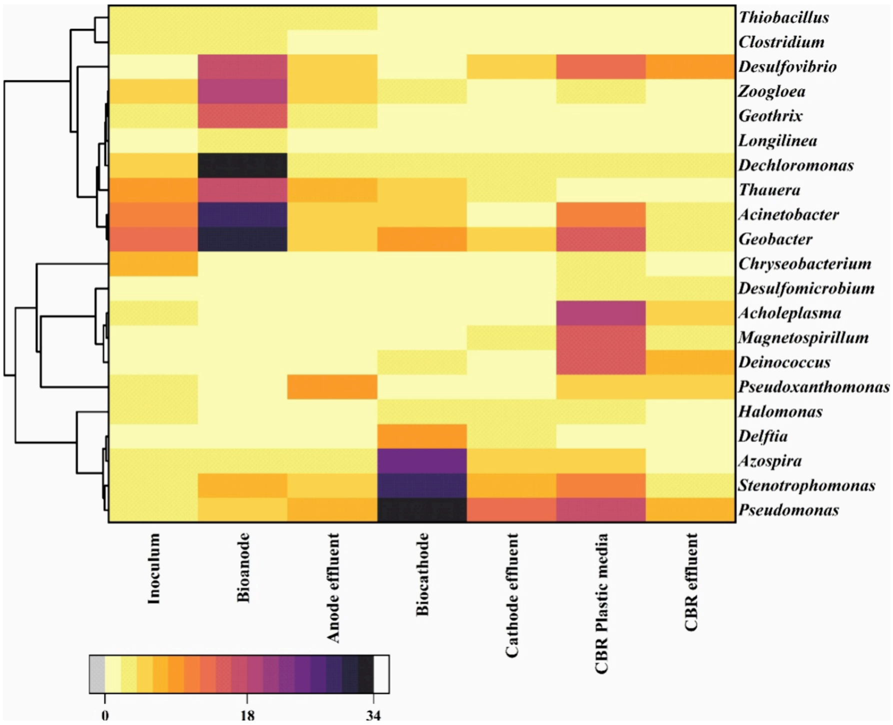


**Figure 7.** Heat map of relative abundance of dominant bacteria at the genus level in the microbial community from the BEC (main) reactor and conventional bioreactor (CBR).

*Azospira* (25%), and *Geobacter* (9%). These genera were significantly enriched compared with the inoculum, where their abundance was less than 8%. This enrichment suggests their active participation in reducing tellurite to $Te^0$, which likely provided these bacteria with energy for growth. *Pseudomonas* can transfer electrons through a mediated process[95] and reduce tellurite to $Te^0$ via intracellular and extracellular mechanisms.[34,35,96] *Stenotrophomonas* is capable of degrading organic compounds extracellularly in microbial fuel cells[55,97] and reducing tellurite to $Te^0$ intracellularly and extracellularly.[37] *Azospira* is known for its extracellular electron transfer ability using its c-type cytochrome to reduce metals in BEC reactors.[98] The high abundance of these species in the biocathode indicates their active role in the bioelectrochemical processes essential for tellurite reduction. The microbial community analysis highlights the significant role of specific bacterial genera in the biocathode and CBR reactor. These microbes are not only crucial for the reduction of tellurite to elemental $Te^0$ but also play important roles in other biochemical processes within the reactors.

## 4. CONCLUSIONS

The increasing demand for critical elements, such as tellurium, necessitates sustainable recovery methods. This study demonstrated efficient removal and conversion of tellurite to elemental $Te^0$ at the biocathode. The shapes of the produced $Te^0$ particles using the mixed culture were nanorods according to the SEM and STEM images coupled with EDX spectra. The biocathode of the BEC reactor achieved extracellular $Te^0$ recovery by using a mixed microbial consortium under anaerobic conditions. This is the first successful demonstration of tellurite removal and elemental $Te^0$ recovery in a biocathode-based BEC reactor. The biocathode of the BEC reactor was able to produce extracellular $Te^0$ nanorods, whereas the CBR produced both intracellular and extracellular $Te^0$ nanorods as determined by the EDX mapping spectra. Despite methanogenesis having a negligible effect on tellurite reduction, sulfate had a minor effect on the reduction of tellurite to elemental $Te^0$. The microbial community analysis provided valuable insights into the functional roles of different bacterial genera within the reactors. Understanding these roles can inform future optimization strategies for bioelectrochemical systems, enhancing their efficiency and effectiveness in removing tellurite and recovering elemental $Te^0$.

BECs are cost-effective, requiring lower energy and chemical inputs, and can be integrated into existing wastewater treatment facilities without a complete overhaul.[99−102] Despite these benefits, BECs face challenges such as metabolic inefficiency, cathode and membrane biofouling, and organic loadings.[103,104] Continued research on optimizing electrodes, exchange membranes, electron transfer stimulation, and engineered microbial species is essential to enhancing BEC performance and their widespread application in industries. By addressing these challenges and leveraging their advantages, BECs have the potential to revolutionize industrial wastewater treatment, providing a sustainable and efficient solution for metal recovery and wastewater management.

## ■ ASSOCIATED CONTENT

### Supporting Information

The Supporting Information is available free of charge at https://pubs.acs.org/doi/10.1021/acsestwater.4c00588.

Sample preparation for SEM and STEM, extraction of DNA, equations for data such as electron distribution, and additional figures and tables to support the methods and results and discussion (PDF)

## AUTHOR INFORMATION

### Corresponding Author

**Youneng Tang** – *Department of Civil and Environmental Engineering, FAMU-FSU College of Engineering, Florida State University, Tallahassee, Florida 32310, United States;* orcid.org/0000-0001-8494-2908; Phone: +1(850)410-6119; Email: ytang@eng.famu.fsu.edu

### Authors

**Benhur K. Asefaw** – *Department of Civil and Environmental Engineering, FAMU-FSU College of Engineering, Florida State University, Tallahassee, Florida 32310, United States*

**Huan Chen** – *National High Magnetic Field Laboratory, Florida State University, Tallahassee, Florida 32310, United States;* orcid.org/0000-0002-6032-6569

Complete contact information is available at: https://pubs.acs.org/10.1021/acsestwater.4c00588

### Notes

The authors declare no competing financial interest.

## ACKNOWLEDGMENTS

This work was supported by the National Science Foundation through award no. 2029682 to Florida State University. The authors greatly thank Dr. Eric Lochner, Dr. Yan Xin, and Mr. Grayson Platt at Florida State University for providing technical support in the SEM, TEM, and STEM imaging, Dr. Jin Gyu Park at the High-Performance Materials Institute, Florida State University for providing help in Raman spectroscopy analysis, and Dr. Amber N. Brown at the Molecular Cloning lab, Florida State University for 16S rRNA sequencing. The SEM work was performed at the Condensed Matter and Material Physics facilities, Florida State University. The TEM work was performed at the Biological Science Imaging Resource, Florida State University using the instrument Hitachi HT7800, which was funded from NSF through grant no. 2017869. A portion of this work was performed at the National High Magnetic Field Laboratory, which is supported by the National Science Foundation Division of Materials Research and Division of Chemistry through DMR-1644779 and the State of Florida.

## REFERENCES

(1) Babula, P.; Adam, V.; Opatrilova, R.; Zehnalek, J.; Havel, L.; Kizek, R.; Lichtfouse, E. Uncommon Heavy Metals, Metalloids and Their Plant Toxicity: A Review. *Environ. Chem. Lett.* **2010**, 275.

(2) Hans Wedepohl, K. The Composition of the Continental Crust. *Geochim. Cosmochim. Acta* **1995**, 1217.

(3) Zannoni, D.; Borsetti, F.; Harrison, J. J.; Turner, R. J. The Bacterial Response to the Chalcogen Metalloids Se and Te. *Adv. Microb. Physiol.* **2007**, 1.

(4) Belzile, N.; Chen, Y. W. Tellurium in the Environment: A Critical Review Focused on Natural Waters, Soils, Sediments and Airborne Particles. *Appl. Geochem.* **2015**, *63*, 83.

(5) Barlaz, M. A.; Chanton, J. P.; Green, R. B. Controls on Landfill Gas Collection Efficiency: Instantaneous and Lifetime Performance. *J. Air Waste Manage. Assoc.* **2009**, *59* (12), 399.

(6) Taylor, D. E. Bacterial Tellurite Resistance. *Trends Microbiol.* **1999**, *7*, 111.

(7) Chasteen, T. G.; Fuentes, D. E.; Tantaleán, J. C.; Vásquez, C. C. Tellurite: History, Oxidative Stress, and Molecular Mechanisms of Resistance: Review Article. *FEMS Microbiol. Rev.* **2009**, *33*, 820.

(8) Makuei, F. M.; Senanayake, G. Extraction of Tellurium from Lead and Copper Bearing Feed Materials and Interim Metallurgical Products – A Short Review. *Miner. Eng.* **2018**, *115*, 79.

(9) Fan, Y.; Yang, Y.; Xiao, Y.; Zhao, Z.; Lei, Y. Recovery of Tellurium from High Tellurium-Bearing Materials by Alkaline Pressure Leaching Process: Thermodynamic Evaluation and Experimental Study. *Hydrometallurgy* **2013**, *139*, 95.

(10) Hosseini, F.; Lashani, E.; Moghimi, H. Simultaneous Bioremediation of Phenol and Tellurite by Lysinibacillus Sp. EBL303 and Characterization of Biosynthesized Te Nanoparticles. *Sci. Rep.* **2023**, *13*, 1243.

(11) Taylor, A. Biochemistry of Tellurium. *Biol. Trace Elem. Res.* **1996**, *55* (3), 231.

(12) Vij, P.; Hardej, D. Evaluation of Tellurium Toxicity in Transformed and Non-Transformed Human Colon Cells. *Environ. Toxicol. Pharmacol.* **2012**, *34* (3), 768.

(13) Hoffmann, J. E. Recovering Selenium and Tellurium from Copper Refinery Slimes. *JOM* **1989**, *41* (7), 33.

(14) Fthenakis, V. M. End-of-Life Management and Recycling of PV Modules. *Energy Policy* **2000**, *28* (14), 1051.

(15) Kavlak, G.; Graedel, T. E. Global Anthropogenic Tellurium Cycles for 1940–2010. *Resour., Conserv. Recycl.* **2013**, *76*, 21.

(16) Calderon, J. L.; Smith, N. M.; Bazilian, M. D.; Holley, E. Critical Mineral Demand Estimates for Low-Carbon Technologies: What Do They Tell Us and How Can They Evolve? *Renewable Sustainable Energy Rev.* **2024**, *189*, No. 113938.

(17) Koketsu, T.; Paul, B.; Wu, C.; Kraehnert, R.; Huang, Y.; Strasser, P. A Lithium–Tellurium Rechargeable Battery with Exceptional Cycling Stability. *J. Appl. Electrochem.* **2016**, *46* (6), 627.

(18) Aspiala, M.; Taskinen, P. Thermodynamic Study of the Ag-Sb-Te System with an Advanced EMF Method. *J. Chem. Thermodyn.* **2016**, *93*, 261.

(19) Malik, I.; Srivastava, T.; Surthi, K. K.; Gayner, C.; Kar, K. K. Enhanced Thermoelectric Performance of N-Type Bi2Te3 Alloyed with Low Cost and Highly Abundant Sulfur. *Mater. Chem. Phys.* **2020**, *255*, No. 123598.

(20) Tang, G.; Qian, Q.; Wen, X.; Zhou, G.; Chen, X.; Sun, M.; Chen, D.; Yang, Z. Phosphate Glass-Clad Tellurium Semiconductor Core Optical Fibers. *J. Alloys Compd.* **2015**, *633*, 1.

(21) Murray, C. B.; Norris, D. J.; Bawendi, M. G. Synthesis and Characterization of Nearly Monodisperse CdE (E = Sulfur, Selenium, Tellurium) Semiconductor Nanocrystallites. *J. Am. Chem. Soc.* **1993**, *115* (19), 8706.

(22) Rellick, J. R.; McMahon, C. J.; Marcus, H. L.; Palmberg, P. W. The Effect of Tellurium on Intergranular Cohesion in Iron. *Metall. Trans.* **1971**, *2* (5), 1492.

(23) Sherwani, A. F.; Usmani, J. A.; Varun. Life Cycle Assessment of Solar PV Based Electricity Generation Systems: A Review. *Renewable and Sustainable Energy Rev.* **2010**, *14*, 540.

(24) U.S. Department of Energy. *Critical Minerals and Materials: U.S. Department of Energy's Strategy to Support Domestic Critical Mineral and Material Supply Chains*; 2021.

(25) Nguyen, V. K.; Choi, W.; Ha, Y.; Gu, Y.; Lee, C.; Park, J.; Jang, G.; Shin, C.; Cho, S. Microbial Tellurite Reduction and Production of Elemental Tellurium Nanoparticles by Novel Bacteria Isolated from Wastewater. *J. Ind. Eng. Chem.* **2019**, *78*, 246.

(26) Xu, L.; Xiong, Y.; Zhang, G.; Zhang, F.; Yang, Y.; Hua, Z.; Tian, Y.; You, J.; Zhao, Z. An Environmental-Friendly Process for Recovery of Tellurium and Copper from Copper Telluride. *J. Cleaner Prod.* **2020**, *272*, No. 122723.

(27) Zhang, T.; Yu, H.; Dai, Y.; Wang, Z.; Yang, D.; Qiu, F. Coupling Adsorption and Reduction for Tellurium Recovery by Hierarchical Porous Nanoscale Zero-Valent Iron (NZVI) /LDOs Composites. *Results Eng.* **2022**, *13*, No. 100356.

(28) Ramos-Ruiz, A.; Field, J. A.; Wilkening, J. V.; Sierra-Alvarez, R. Recovery of Elemental Tellurium Nanoparticles by the Reduction of Tellurium Oxyanions in a Methanogenic Microbial Consortium. *Environ. Sci. Technol.* **2016**, *50* (3), 1492.

(29) Wadgaonkar, S. L.; Mal, J.; Nancharaiah, Y. V.; Maheshwari, N. O.; Esposito, G.; Lens, P. N. L. Formation of Se(0), Te(0), and Se(0)−Te(0) Nanostructures during Simultaneous Bioreduction of Selenite and Tellurite in a UASB Reactor. *Appl. Microbiol. Biotechnol.* **2018**, *102* (6), 2899.
(30) Turner, R. J.; Borghese, R.; Zannoni, D. Microbial Processing of Tellurium as a Tool in Biotechnology. *Biotechnol. Adv.* **2012**, *30*, 954.
(31) Baesman, S. M.; Bullen, T. D.; Dewald, J.; Zhang, D.; Curran, S.; Islam, F. S.; Beveridge, T. J.; Oremland, R. S. Formation of Tellurium Nanocrystals during Anaerobic Growth of Bacteria That Use Te Oxyanions as Respiratory Electron Acceptors. *Appl. Environ. Microbiol.* **2007**, *73* (7), 2135.
(32) Baesman, S. M.; Stolz, J. F.; Kulp, T. R.; Oremland, R. S. Enrichment and Isolation of Bacillus Beveridgei Sp. Nov., a Facultative Anaerobic Haloalkaliphile from Mono Lake, California, That Respires Oxyanions of Tellurium, Selenium, and Arsenic. *Extremophiles* **2009**, *13* (4), 695.
(33) Borghese, R.; Baccolini, C.; Francia, F.; Sabatino, P.; Turner, R. J.; Zannoni, D. Reduction of Chalcogen Oxyanions and Generation of Nanoprecipitates by the Photosynthetic Bacterium Rhodobacter Capsulatus. *J. Hazard. Mater.* **2014**, *269*, 24.
(34) Chua, S. L.; Sivakumar, K.; Rybtke, M.; Yuan, M.; Andersen, J. B.; Nielsen, T. E.; Givskov, M.; Tolker-Nielsen, T.; Cao, B.; Kjelleberg, S.; Yang, L. C-Di-GMP Regulates Pseudomonas Aeruginosa Stress Response to Tellurite during Both Planktonic and Biofilm Modes of Growth. *Sci. Rep.* **2015**, *5*, 10052.
(35) Peng, W.; Wang, Y.; Fu, Y.; Deng, Z.; Lin, S.; Liang, R. Characterization of the Tellurite-Resistance Properties and Identification of the Core Function Genes for Tellurite Resistance in Pseudomonas Citronellolis Sjte-3. *Microorganisms* **2022**, *10* (1), 95.
(36) Bonificio, W. D.; Clarke, D. R. Bacterial Recovery and Recycling of Tellurium from Tellurium-Containing Compounds by Pseudoalteromonas Sp. EPR3. *J. Appl. Microbiol.* **2014**, *117* (5), 1293.
(37) Pages, D.; Rose, J.; Conrod, S.; Cuine, S.; Carrier, P.; Heulin, T.; Achouak, W.; Ward, N. Heavy Metal Tolerance in Stenotrophomonas Maltophilia. *PLoS One* **2008**, *3* (2), No. e1539.
(38) Narayanan, K. B.; Sakthivel, N. Biological Synthesis of Metal Nanoparticles by Microbes. *Adv. Colloid Interface Sci.* **2010**, *156*, 1.
(39) Mal, J.; Nancharaiah, Y. V.; Maheshwari, N.; van Hullebusch, E. D.; Lens, P. N. L. Continuous Removal and Recovery of Tellurium in an Upflow Anaerobic Granular Sludge Bed Reactor. *J. Hazard. Mater.* **2017**, *327*, 79.
(40) Ramos-Ruiz, A.; Sesma-Martin, J.; Sierra-Alvarez, R.; Field, J. A. Continuous Reduction of Tellurite to Recoverable Tellurium Nanoparticles Using an Upflow Anaerobic Sludge Bed (UASB) Reactor. *Water Res.* **2017**, *108*, 189.
(41) Ramos-Ruiz, A.; Zeng, C.; Sierra-Alvarez, R.; Teixeira, L. H.; Field, J. A. Microbial Toxicity of Ionic Species Leached from the II-VI Semiconductor Materials, Cadmium Telluride (CdTe) and Cadmium Selenide (CdSe). *Chemosphere* **2016**, *162*, 131.
(42) Oremland, R. S.; Baseman, S.; Fellowes, J.; Pearce, C. Nanoparticles Formed from Bacterial Oxyanion Reduction of Toxic Group 15 and 16 Metalloids. *Microb. Met. Metalloid Metab.* **2011**, 297−319.
(43) Shakibaie, M.; Khorramizadeh, M. R.; Al Faramarzi, M.; Sabzevari, O.; Shahverdi, A. R. Biosynthesis and Recovery of Selenium Nanoparticles and the Effects on Matrix Metalloproteinase-2 Expression. *Biotechnol. Appl. Biochem.* **2010**, *56* (1), 7.
(44) Sonkusre, P.; Nanduri, R.; Gupta, P.; Cameotra, S. S. Improved Extraction of Intracellular Biogenic Selenium Nanoparticles and Their Specificity for Cancer Chemoprevention. *J. Nanomed. Nanotechnol.* **2014**, *5* (2), No. 1000194.
(45) Logan, B. E.; Rabaey, K. Conversion of Wastes into Bioelectricity and Chemicals by Using Microbial Electrochemical Technologies. *Science* **2012**, *337*, 686.
(46) Zhang, Z.; Chen, G.; Tang, Y. Towards Selenium Recovery: Biocathode Induced Selenate Reduction to Extracellular Elemental Selenium Nanoparticles. *Chem. Eng. J.* **2018**, *351*, 1095.
(47) Goglio, A.; Tucci, M.; Rizzi, B.; Colombo, A.; Cristiani, P.; Schievano, A. Microbial Recycling Cells (MRCs): A New Platform of Microbial Electrochemical Technologies Based on Biocompatible Materials, Aimed at Cycling Carbon and Nutrients in Agro-Food Systems. *Sci. Total Environ.* **2019**, *649*, 1349.
(48) Zhang, Z.; Sarkar, D.; Li, L.; Datta, R. Contaminant Removal and Resource Recovery in Bioelectrochemical Wastewater Treatment. *Curr. Pollut. Rep.* **2022**, *8*, 159.
(49) Amanze, C.; Zheng, X.; Man, M.; Yu, Z.; Ai, C.; Wu, X.; Xiao, S.; Xia, M.; Yu, R.; Wu, X.; Shen, L.; Liu, Y.; Li, J.; Dolgor, E.; Zeng, W. Recovery of Heavy Metals from Industrial Wastewater Using Bioelectrochemical System Inoculated with Novel Castellaniella Species. *Environ. Res.* **2022**, *205*, No. 112467.
(50) Sravan, J. S.; Mohan, S. V. Bioelectrocatalytic Reduction of Tellurium Oxyanions toward Their Cathodic Recovery: Concentration Dependence and Anodic Electrogenic Activity. *ACS Environ. Sci. Technol. Water* **2022**, *2*, 40.
(51) Nancharaiah, Y. V.; Mohan, S. V.; Lens, P. N. L. Metals Removal and Recovery in Bioelectrochemical Systems: A Review. *Bioresour. Technol.* **2015**, *195*, 102.
(52) Li, M.; Zhou, M.; Tian, X.; Tan, C.; McDaniel, C. T.; Hassett, D. J.; Gu, T. Microbial Fuel Cell (MFC) Power Performance Improvement through Enhanced Microbial Electrogenicity. *Biotechnol. Adv.* **2018**, *36*, 1316.
(53) Syed, Z.; Sogani, M.; Dongre, A.; Kumar, A.; Sonu, K.; Sharma, G.; Gupta, A. B. Bioelectrochemical Systems for Environmental Remediation of Estrogens: A Review and Way Forward. *Sci. Total Environ.* **2021**, *780*, No. 146544.
(54) Tandukar, M.; Huber, S. J.; Onodera, T.; Pavlostathis, S. G. Biological Chromium(VI) Reduction in the Cathode of a Microbial Fuel Cell. *Environ. Sci. Technol.* **2009**, *43* (21), 8159.
(55) Zhang, Z.; Asefaw, B. K.; Xiong, Y.; Chen, H.; Tang, Y. Evidence and Mechanisms of Selenate Reduction to Extracellular Elemental Selenium Nanoparticles on the Biocathode. *Environ. Sci. Technol.* **2022**, *56* (22), 16259−16270.
(56) Huang, L.; Chai, X.; Chen, G.; Logan, B. E. Effect of Set Potential on Hexavalent Chromium Reduction and Electricity Generation from Biocathode Microbial Fuel Cells. *Environ. Sci. Technol.* **2011**, *45*, 5025.
(57) Huang, L.; Yao, B.; Wu, D.; Quan, X. Complete Cobalt Recovery from Lithium Cobalt Oxide in Self-Driven Microbial Fuel Cell - Microbial Electrolysis Cell Systems. *J. Power Sources* **2014**, 54.
(58) Kaushik, A.; Singh, A. Metal Removal and Recovery Using Bioelectrochemical Technology: The Major Determinants and Opportunities for Synchronic Wastewater Treatment and Energy Production. *J. Environ. Manage.* **2020**, No. 110826.
(59) Leong, J. X.; Daud, W. R. W.; Ghasemi, M.; Liew, K. B.; Ismail, M. Ion Exchange Membranes as Separators in Microbial Fuel Cells for Bioenergy Conversion: A Comprehensive Review. *Renewable Sustainable Energy Rev.* **2013**, *28*, 575.
(60) Chacón-Carrera, R. A.; López-Ortiz, A.; Collins-Martínez, V.; Meléndez-Zaragoza, M. J.; Salinas-Gutiérrez, J.; Espinoza-Hicks, J. C.; Ramos-Sánchez, V. H. Assessment of Two Ionic Exchange Membranes in a Bioelectrochemical System for Wastewater Treatment and Hydrogen Production. *Int. J. Hydrogen Energy* **2019**, *44*, 12339.
(61) Turner, R. J.; Weiner, J. H.; Taylor, D. E. Use of Diethyldithiocarbamate for Quantitative Determination of Tellurite Uptake by Bacteria. *Anal. Biochem.* **1992**, *204* (2), 292.
(62) Pylro, V. S.; Roesch, L. F. W.; Morais, D. K.; Clark, I. M.; Hirsch, P. R.; Tótola, M. R. Data Analysis for 16S Microbial Profiling from Different Benchtop Sequencing Platforms. *J. Microbiol. Methods* **2014**, *107*, 30.
(63) Ionescu, D.; Overholt, W. A.; Lynch, M. D. J.; Neufeld, J. D.; Naqib, A.; Green, S. J. Microbial Community Analysis Using High-Throughput Amplicon Sequencing. *Man. Environ. Microbiol.* **2015**, 2.
(64) Caporaso, J. G.; Kuczynski, J.; Stombaugh, J.; Bittinger, K.; Bushman, F. D.; Costello, E. K.; Fierer, N.; Pẽa, A. G.; Goodrich, J. K.; Gordon, J. I.; Huttley, G. A.; Kelley, S. T.; Knights, D.; Koenig, J.

E.; Ley, R. E.; Lozupone, C. A.; McDonald, D.; Muegge, B. D.; Pirrung, M.; Reeder, J.; Sevinsky, J. R.; Turnbaugh, P. J.; Walters, W. A.; Widmann, J.; Yatsunenko, T.; Zaneveld, J.; Knight, R. QIIME Allows Analysis of High-Throughput Community Sequencing Data. *Nat. Methods* **2010**, *7*, 335.

(65) Barter, R. L.; Yu, B. Superheat: An R Package for Creating Beautiful and Extendable Heatmaps for Visualizing Complex Data. *J. Comput. Graphical Stat.* **2018**, *27* (4), 910.

(66) Bouroushian, M. Chalcogens and Metal Chalcogenides; In *Electrochemistry of Metal Chalcogenides* 2010. Springer .

(67) Bajaj, M.; Winter, J. Se (IV) Triggers Faster Te (IV) Reduction by Soil Isolates of Heterotrophic Aerobic Bacteria: Formation of Extracellular SeTe Nanospheres. *Microb. Cell Fact.* **2014**, *13*, 168.

(68) Zhang, Z.; Adedeji, I.; Chen, G.; Tang, Y. Chemical-Free Recovery of Elemental Selenium from Selenate-Contaminated Water by a System Combining a Biological Reactor, a Bacterium-Nanoparticle Separator, and a Tangential Flow Filter. *Environ. Sci. Technol.* **2018**, *52* (22), 13231.

(69) Zhong, Z.; Li, W.; Xing, W.; Xu, N. Crossflow Filtration of Nanosized Catalysts Suspension Using Ceramic Membranes. *Sep. Purif. Technol.* **2011**, *76*, 223.

(70) Anders, C. B.; Baker, J. D.; Stahler, A. C.; Williams, A. J.; Sisco, J. N.; Trefry, J. C.; Wooley, D. P.; Sizemore, I. E. P. Tangential Flow Ultrafiltration: A "Green" Method for the Size Selection and Concentration of Colloidal Silver Nanoparticles. *J. Vis. Exp.* **2012**, 4167.

(71) Basnet, R.; Doha, M. H.; Hironaka, T.; Pandey, K.; Davari, S.; Welch, K. M.; Churchill, H. O. H.; Hu, J. Growth and Strain Engineering of Trigonal Te for Topological Quantum Phases in Non-Symmorphic Chiral Crystals. *Crystals* **2019**, *9* (10), 486.

(72) Brodsky, M. H.; Gambino, R. J.; Smith, J. E.; Yacoby, Y. The Raman Spectrum of Amorphous Tellurium. *Phys. status solidi* **1972**, *52* (2), 609.

(73) Liu, J. W.; Xu, J.; Hu, W.; Yang, J. L.; Yu, S. H. Systematic Synthesis of Tellurium Nanostructures and Their Optical Properties: From Nanoparticles to Nanorods, Nanowires, and Nanotubes. *ChemNanoMat* **2016**, *2* (3), 167.

(74) Baesman, S. M.; Stolz, J. F.; Kulp, T. R.; Oremland, R. S. Enrichment and Isolation of Bacillus Beveridgei Sp. Nov., a Facultative Anaerobic Haloalkaliphile from Mono Lake, California, That Respires Oxyanions of Tellurium, Selenium, and Arsenic. *Extremophiles* **2009**, *13*, 695.

(75) Zare, B.; Faramarzi, M. A.; Sepehrizadeh, Z.; Shakibaie, M.; Rezaie, S.; Shahverdi, A. R. Biosynthesis and Recovery of Rod-Shaped Tellurium Nanoparticles and Their Bactericidal Activities. *Mater. Res. Bull.* **2012**, *47* (11), 3719.

(76) Nguyen, T. T. H.; Kikuchi, T.; Tokunaga, T.; Iyoda, S.; Iguchi, A. Diversity of the Tellurite Resistance Gene Operon in Escherichia Coli. *Front. Microbiol.* **2021**, No. 681175.

(77) Busalmen, J. P.; Esteve-Núñez, A.; Berná, A.; Feliu, J. M. C-Type Cytochromes Wire Electricity-Producing Bacteria to Electrodes. *Angew. Chem. - Int. Ed.* **2008**, *47* (26), 4874.

(78) Wu, J. F.; Xu, M. Q.; Zhao, G. C. Graphene-Based Modified Electrode for the Direct Electron Transfer of Cytochrome c and Biosensing. *Electrochem. Commun.* **2010**, *12* (1), 175.

(79) Zou, L.; Zhu, F.; Long, Z.-E.; Huang, Y. Bacterial Extracellular Electron Transfer: A Powerful Route to the Green Biosynthesis of Inorganic Nanomaterials for Multifunctional Applications. *J. Nanobiotechnol.* **2021**, 120.

(80) Li, D. B.; Cheng, Y. Y.; Wu, C.; Li, W. W.; Li, N.; Yang, Z. C.; Tong, Z. H.; Yu, H. Q. Selenite Reduction by Shewanella Oneidensis MR-1 Is Mediated by Fumarate Reductase in Periplasm. *Sci. Rep.* **2014**, *4*, 3735.

(81) Von Canstein, H.; Ogawa, J.; Shimizu, S.; Lloyd, J. R. Secretion of Flavins by Shewanella Species and Their Role in Extracellular Electron Transfer. *Appl. Environ. Microbiol.* **2008**, *74* (3), 615.

(82) Lefebvre, O.; Al-Mamun, A.; Ng, H. Y. A Microbial Fuel Cell Equipped with a Biocathode for Organic Removal and Denitrification. *Water Sci. Technol.* **2008**, *58* (4), 881.

(83) Ki, D.; Popat, S. C.; Torres, C. I. Reduced Overpotentials in Microbial Electrolysis Cells through Improved Design, Operation, and Electrochemical Characterization. *Chem. Eng. J.* **2016**, *287*, 181.

(84) Puig, S.; Coma, M.; Desloover, J.; Boon, N.; Colprim, J.; Balaguer, M. D. Autotrophic Denitrification in Microbial Fuel Cells Treating Low Ionic Strength Waters. *Environ. Sci. Technol.* **2012**, *46* (4), 2309.

(85) Bond, D. R.; Lovley, D. R. Electricity Production by Geobacter Sulfurreducens Attached to Electrodes. *Appl. Environ. Microbiol.* **2003**, *69* (3), 1548.

(86) Chang, C. C.; Chen, Y. C.; Yu, C. P. Microbial Community Dynamics in Electroactive Biofilms across Time under Different Applied Anode Potentials. *Sustainable Environ. Res.* **2022**, *32* (1), 19.

(87) Freguia, S.; Tsujimura, S.; Kano, K. Electron Transfer Pathways in Microbial Oxygen Biocathodes. *Electrochim. Acta* **2010**, *55* (3), 813.

(88) Yang, N.; Zhan, G.; Li, D.; Wang, X.; He, X.; Liu, H. Complete Nitrogen Removal and Electricity Production in Thauera-Dominated Air-Cathode Single Chambered Microbial Fuel Cell. *Chem. Eng. J.* **2019**, *356*, 506.

(89) Eddie, B. J.; Glaven, S. M. Electrified Biofilms: A Special Issue on Microbial Electrochemistry. *Biofilm* **2021**, No. 100062.

(90) Bond, D. R.; Lovley, D. R. Evidence for Involvement of an Electron Shuttle in Electricity Generation by Geothrix Fermentans. *Appl. Environ. Microbiol.* **2005**, *71* (4), 2186.

(91) Obata, O.; Salar-Garcia, M. J.; Greenman, J.; Kurt, H.; Chandran, K.; Ieropoulos, I. Development of Efficient Electroactive Biofilm in Urine-Fed Microbial Fuel Cell Cascades for Bioelectricity Generation. *J. Environ. Manage.* **2020**, *258*, No. 109992.

(92) Vinther, O.; Freundt, E. A. Ultrastructural Localization of Tellurite Reduction in Acholeplasma Species. *Acta Pathol. Microbiol. Scand., Sect. B: Microbiol. Immunol.* **1977**, *85* (3), 184.

(93) Anaganti, N.; Basu, B.; Gupta, A.; Joseph, D.; Apte, S. K. Depletion of Reduction Potential and Key Energy Generation Metabolic Enzymes Underlies Tellurite Toxicity in Deinococcus Radiodurans. *Proteomics* **2015**, *15* (1), 89.

(94) Tanaka, M.; Arakaki, A.; Staniland, S. S.; Matsunaga, T. Simultaneously Discrete Biomineralization of Magnetite and Tellurium Nanocrystals in Magnetotactic Bacteria. *Appl. Environ. Microbiol.* **2010**, *76* (16), 5526.

(95) Allam, F.; Elnouby, M.; Sabry, S. A.; El-Khatib, K. M.; El-Badan, D. E. Optimization of Factors Affecting Current Generation, Biofilm Formation and Rhamnolipid Production by Electroactive Pseudomonas Aeruginosa FA17. *Int. J. Hydrogen Energy* **2021**, *46* (20), 11419.

(96) Rajwade, J. M.; Paknikar, K. M. Bioreduction of Tellurite to Elemental Tellurium by Pseudomonas Mendocina MCM B-180 and Its Practical Application. *Hydrometallurgy* **2003**, *71*, 243.

(97) Venkidusamy, K.; Megharaj, M. Identification of Electrode Respiring, Hydrocarbonoclastic Bacterial Strain Stenotrophomonas Maltophilia MK2 Highlights the Untapped Potential for Environmental Bioremediation. *Front. Microbiol.* **2016**, *7*, No. 1965.

(98) Becerril-Varela, K.; Serment-Guerrero, J. H.; Manzanares-Leal, G. L.; Ramírez-Durán, N.; Guerrero-Barajas, C. Generation of Electrical Energy in a Microbial Fuel Cell Coupling Acetate Oxidation to Fe3+ Reduction and Isolation of the Involved Bacteria. *World J. Microbiol. Biotechnol.* **2021**, *37* (6), 104.

(99) Malaeb, L.; Katuri, K. P.; Logan, B. E.; Maab, H.; Nunes, S. P.; Saikaly, P. E. A Hybrid Microbial Fuel Cell Membrane Bioreactor with a Conductive Ultrafiltration Membrane Biocathode for Wastewater Treatment. *Environ. Sci. Technol.* **2013**, 11821.

(100) Aguirre-Sierra, A.; Bacchetti-De Gregoris, T.; Berná, A.; Salas, J. J.; Aragón, C.; Esteve-Núñez, A. Microbial Electrochemical Systems Outperform Fixed-Bed Biofilters in Cleaning up Urban Wastewater. *Environ. Sci. Water Res. Technol.* **2016**, 984.

(101) Tejedor-Sanz, S.; Ortiz, J. M.; Esteve-Núñez, A. Merging Microbial Electrochemical Systems with Electrocoagulation Pretreatment for Achieving a Complete Treatment of Brewery Wastewater. *Chem. Eng. J.* **2017**, 1068.


https://doi.org/10.1021/acsestwater.4c00588
ACS EST Water 2024, 4, 4579−4590

(102) Naradasu, D.; Long, X.; Okamoto, A.; Miran, W. Bioelectrochemical Systems: Principles and Applications. In *Bioelectrochemical Systems: Vol.1 Principles and Processes*; Springer 2021, DOI: .

(103) Leang, C.; Malvankar, N. S.; Franks, A. E.; Nevin, K. P.; Lovley, D. R. Engineering Geobacter Sulfurreducens to Produce a Highly Cohesive Conductive Matrix with Enhanced Capacity for Current Production. *Energy Environ. Sci.* **2013**, 1901.

(104) Yong, X.-Y.; Feng, J.; Chen, Y.-L.; Shi, D.-Y.; Xu, Y.-S.; Zhou, J.; Wang, S.-Y.; Xu, L.; Yong, Y.-C.; Sun, Y.-M.; Shi, C.-L.; OuYang, P.-K.; Zheng, T. Enhancement of Bioelectricity Generation by Cofactor Manipulation in Microbial Fuel Cell. *Biosens. Bioelectron.* **2014**, 19.